Synthesis of STW zeolite using imidazolium-based dications of varying length

Peng Lu, Luis Gómez-Hortigüela, Lei Xu, Miguel A. Camblor

Supporting Information

Index:

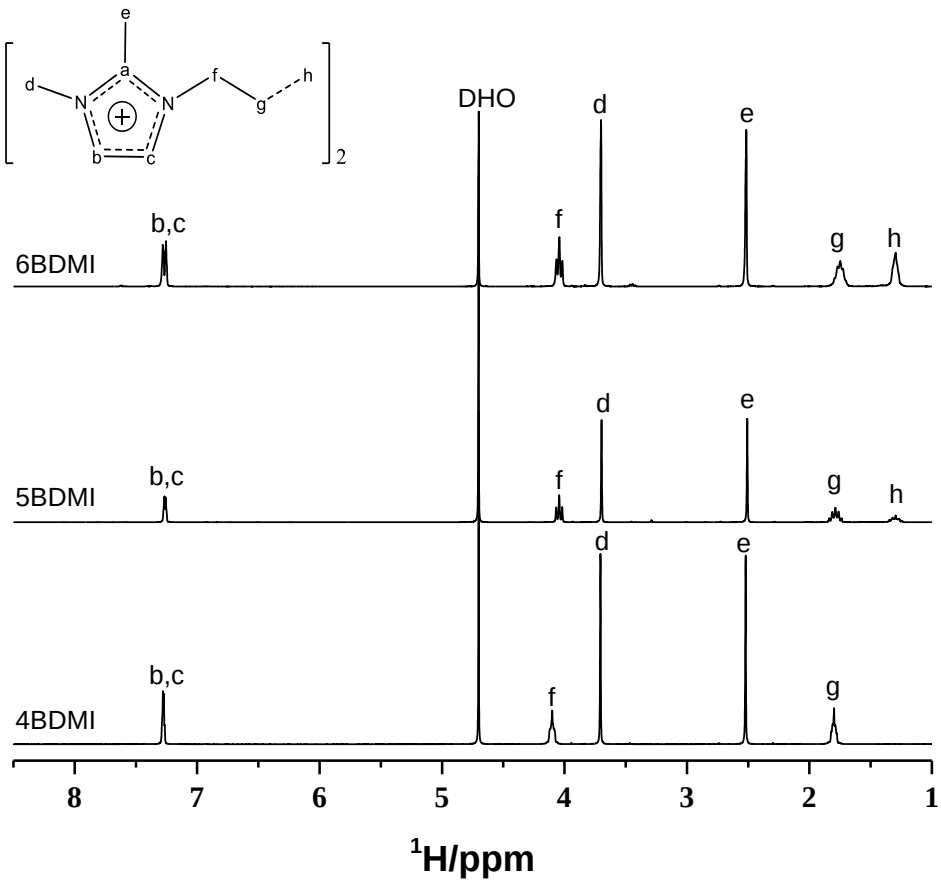

Figure S1. ^{1}H NMR in D_2O of the three organic dications used in this work.

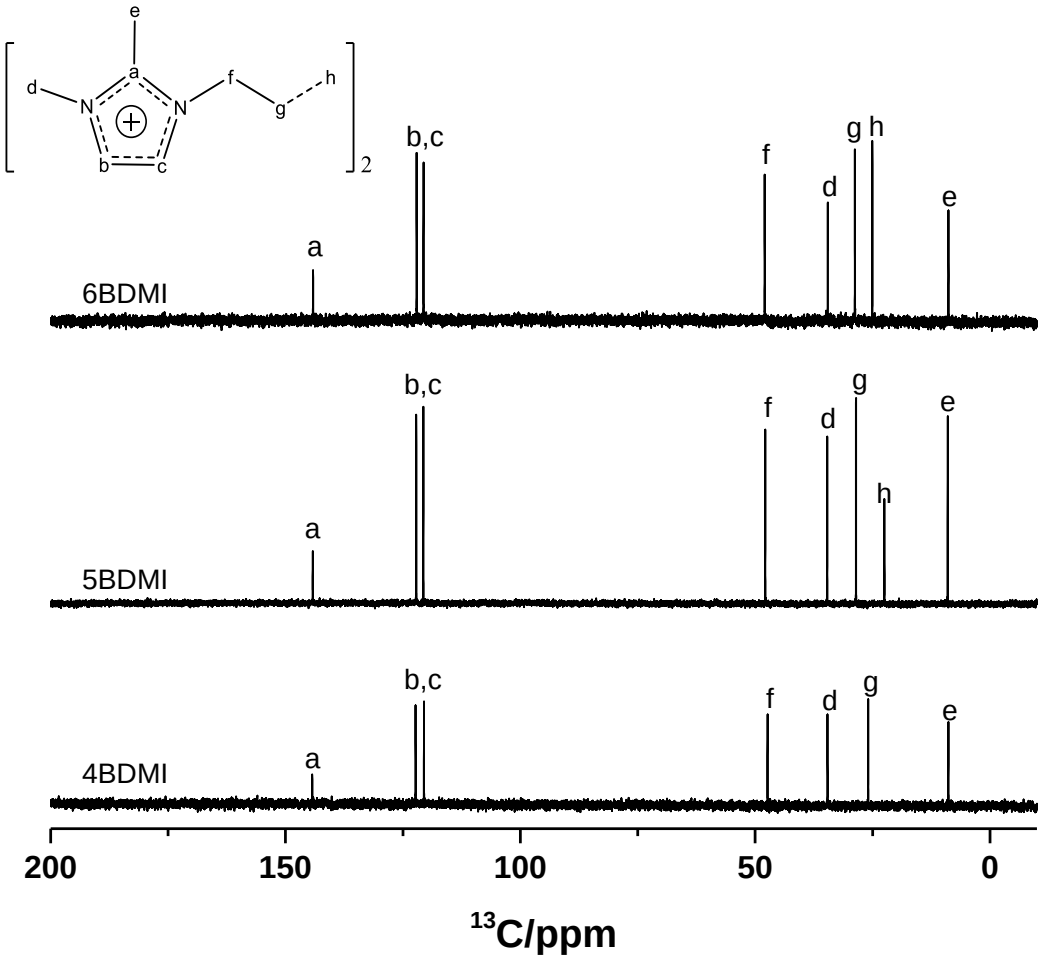

Figure S2. ^{13}C NMR in D_2O of the three organic dications used in this work.

Table S1 Synthesis results for pure silica and germanosilicate zeolites using *n*BDMI [*n*=4,5,6].

SDA	Ge/T(Si+Ge)	Temperature (℃)	H_2O/(Si+Ge)	time(days)	product
4BDMI	0	175	5	3	MTW+STW
				7	STW
			3	1	Amorphous(STW)
				3	STW
				7	STW
		150	10	3	Amorphous
				7	Amorphous+MTW
				14	MTW(amorphous)
	0.05	175	5	2	STW
				4	STW
				6	STW
	0.5	150	15	3	STW
				5	STW
				7	STW
5BDMI	0	175	5	2	MTW
				5	MTW
				9	MTW
			3	1	Amorphous
				3	MTW
				7	MTW+STW
	0.5	150	5	1	STW
				4	STW
				6	STW
6BDMI	0	175	3	1	MTW
				5	MTW
				9	MTW
		150	5	3	Amorphous(MTW)
				5	MTW
				9	MTW
	0.1	175	5	1	Unknown
				3	Unknown
				7	Unknown
	0.25			1	Unknown
				3	Unknown
				7	Unknown
	0.5		15	3	STW (GeO_2+amorphous)
				5	STW (GeO_2+amorphous)
				7	STW (amorphous)
				10	STW (GeO_2+amorphous)

Products in parentheses denote minor phases.

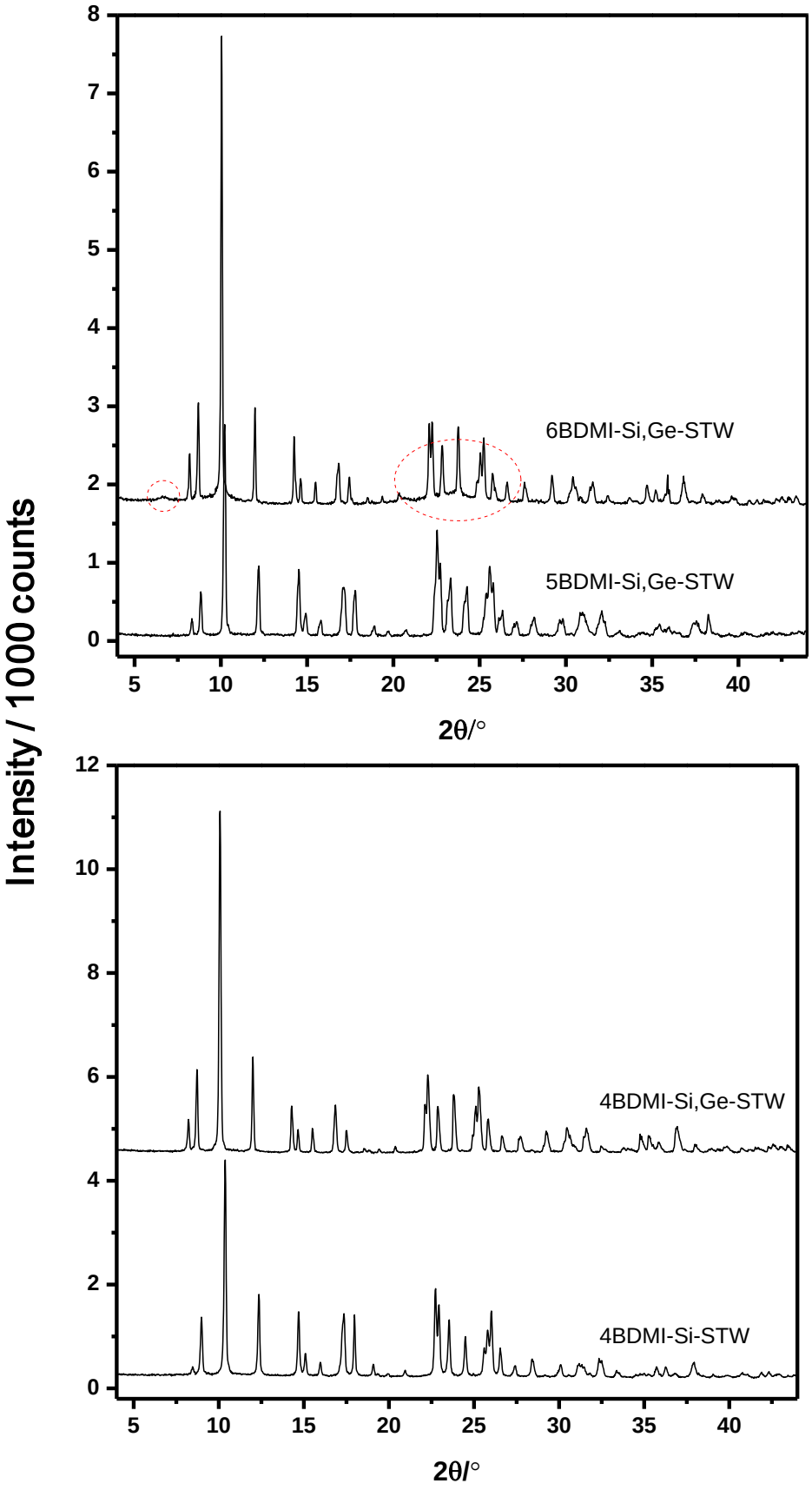

Figure S3. XRD patterns of as-made (germano)silicate STW zeolites, Ge_f (from bottom to top) = 0, 0.5, 0.1 and 0.5. Features enclosed in red lines indicate the presence of an amorphous phase.

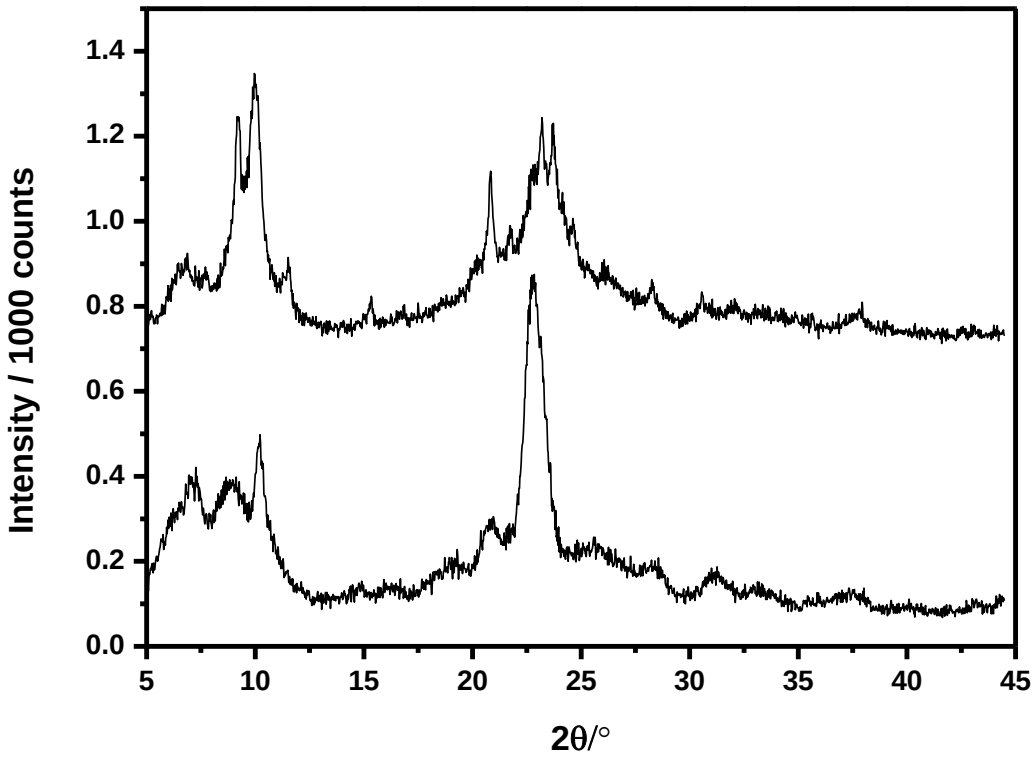

Figure S4. XRD patterns of the products obtained using 6BDMI with gel Ge_f = 0.1(bottom) and 0.25 (top).

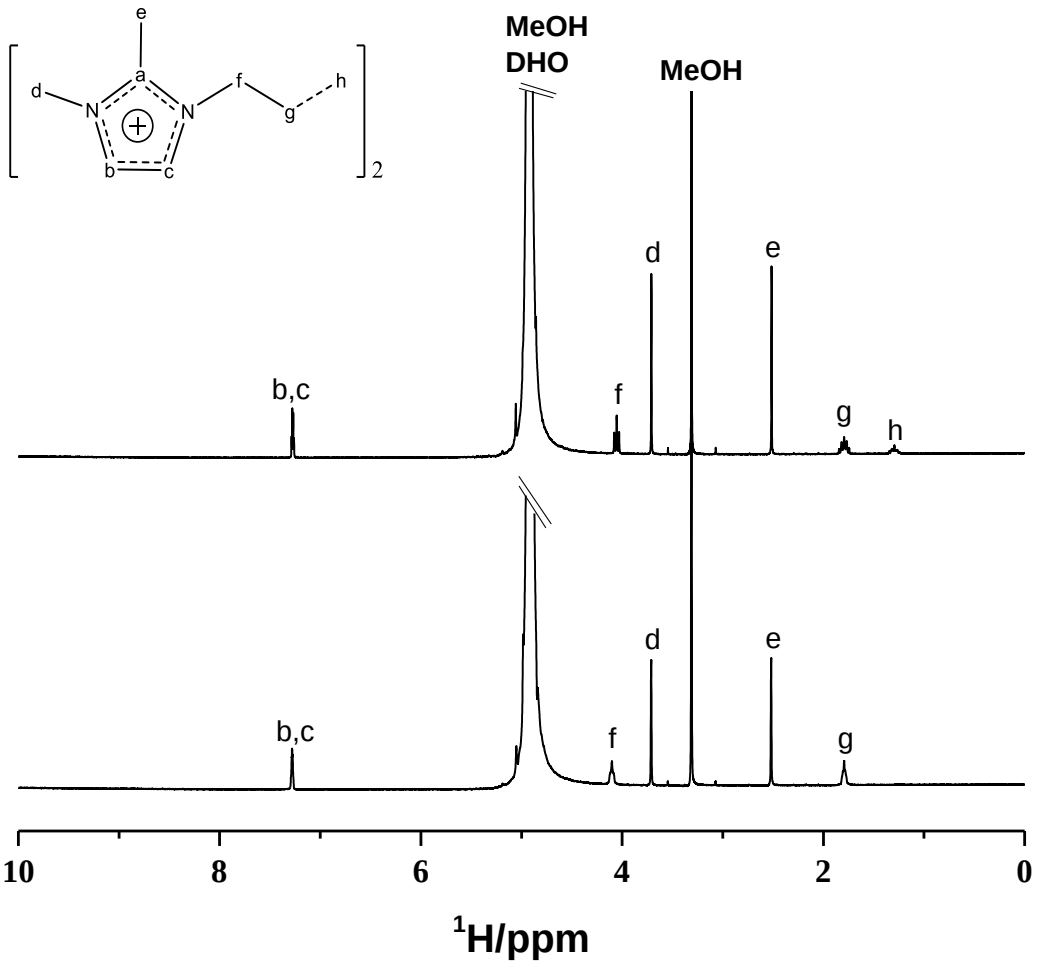

Figure S5. ^{1}H NMR spectra of the zeolites dissolved in HF/D_2O (see reported procedure[1]): (bottom) 4BDMI-Si-STW and (top) 5BDMI-Si,Ge-STW.

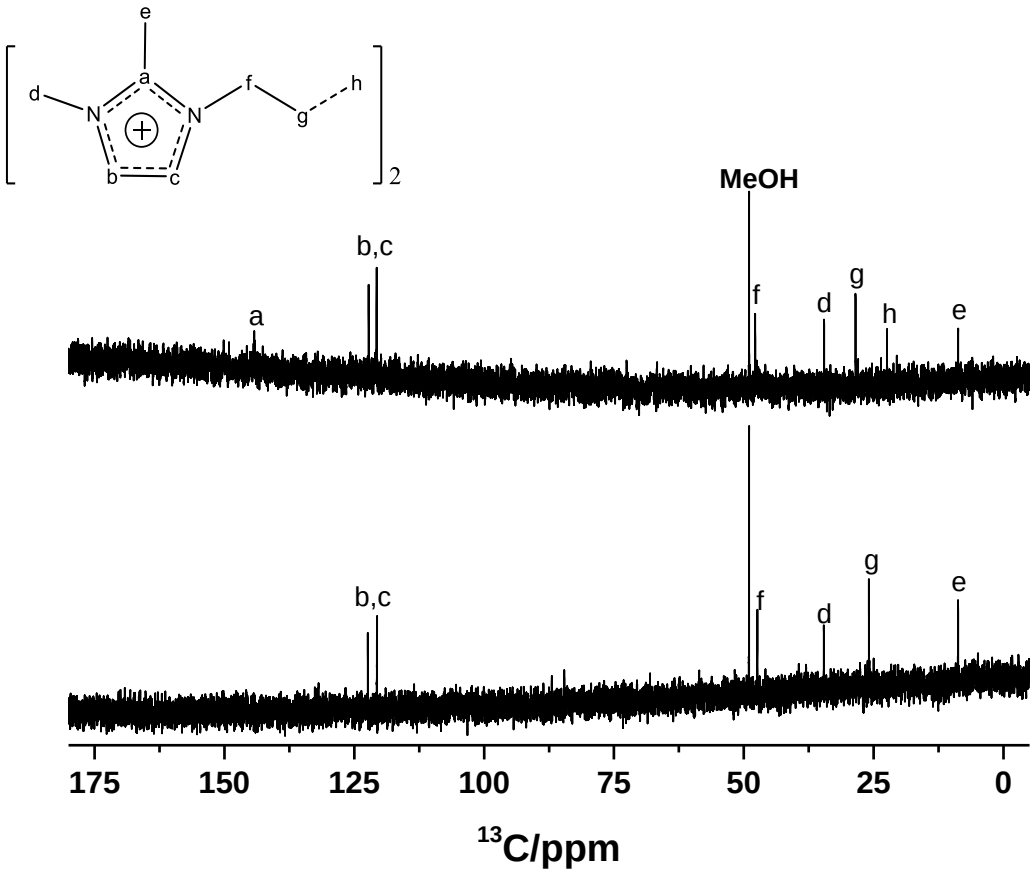

Figure S6. ^{13}C NMR spectra of the the zeolites dissolved in HF/D_2O (see reported procedure in reference [1]): (bottom) 4BDMI-Si-STW and (top) 5BDMI-Si,Ge-STW.

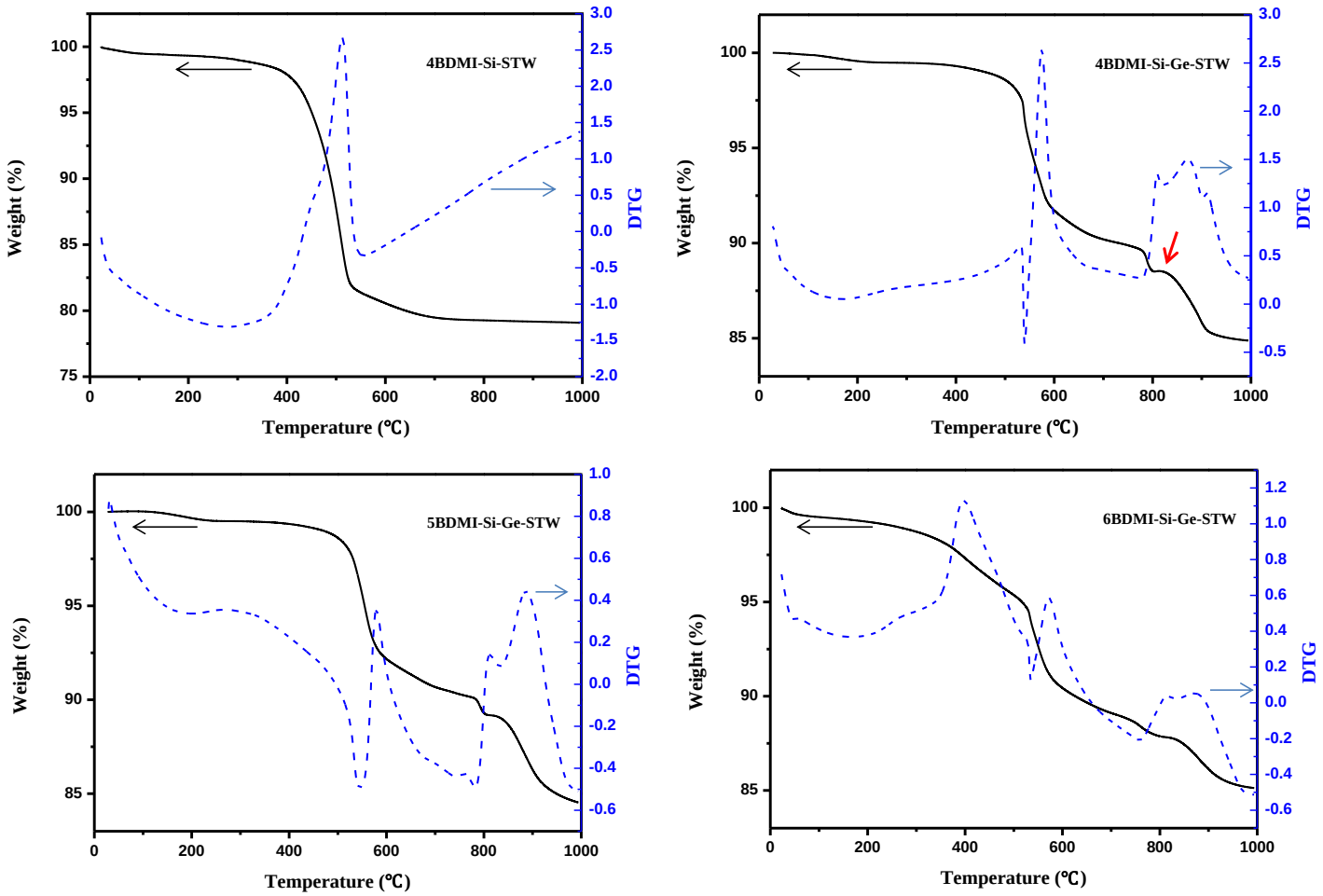

Figure S7. Thermogravimetry (TG) and derivative thermogravimetry (DTG) in flowing air of 4BDMI-Si-STW, 4BDMI-Si,Ge-STW, 5BDMI-Si,Ge-STW and 6BDMI-Si,Ge-STW. The red arrow points to a weight-gaining step in 4BDMI-Si,Ge-STW that shall correspond to reoxidation of previously reduced GeO_2 (see main text and reference [2]).

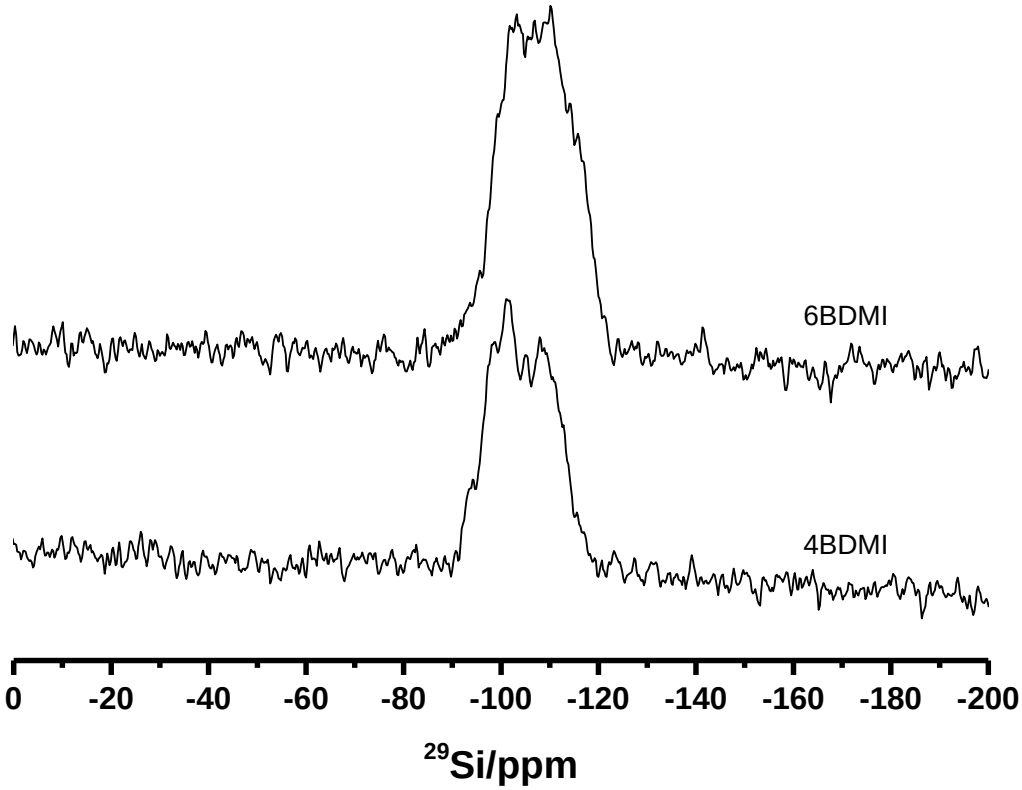

Figure S8. ^{29}Si MAS NMR spectra of two as-made germanosilicate STW zeolites.

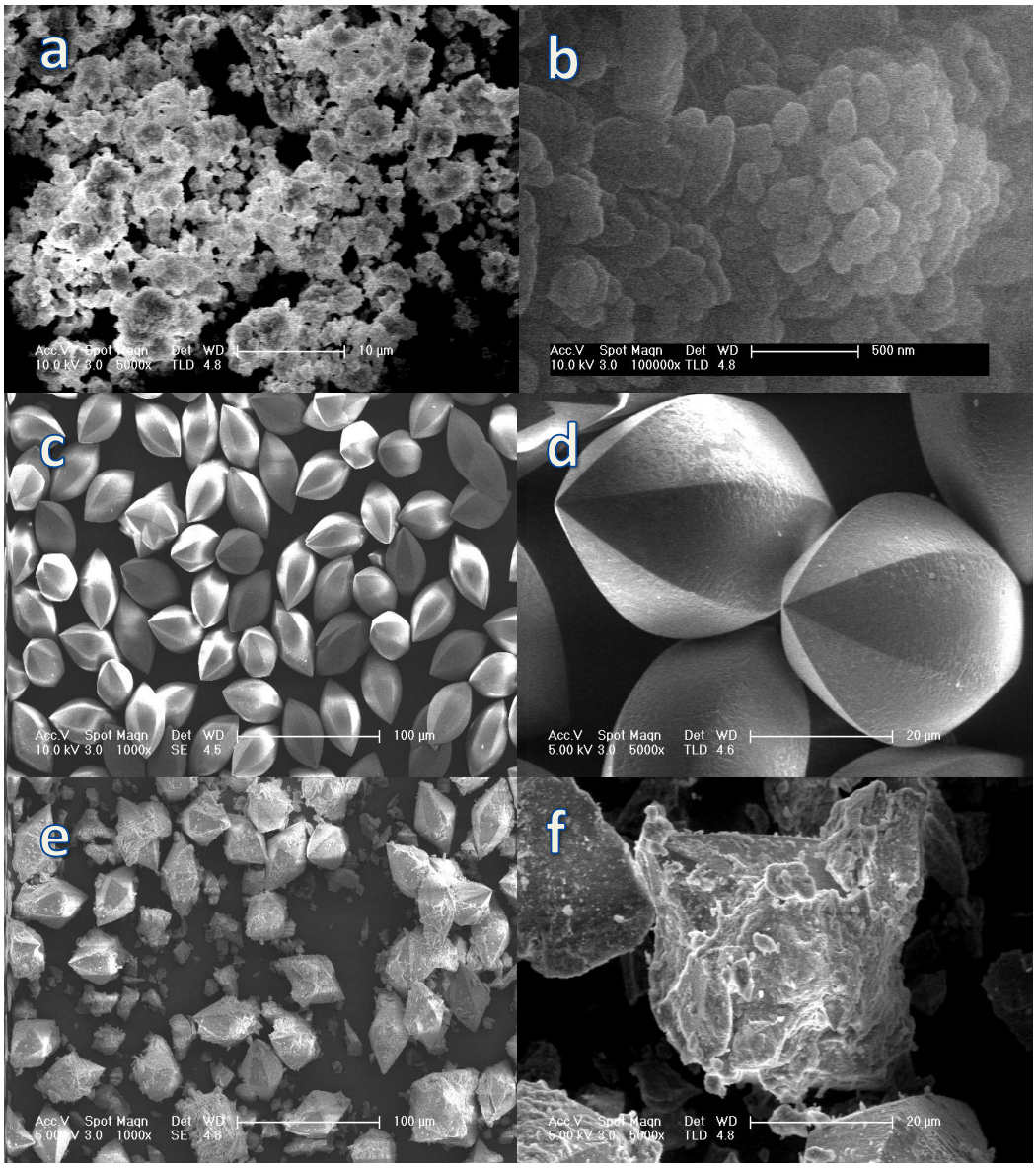

Figure S9. FE-SEM images of 4BDMI-Si-STW zeolites (a, b), 4BDMI-Si,Ge-STWzeolites (c, d) and 6BDMI-Si,Ge-STW zeolites(e,f).

Rietveld refinement of 4BDMI- Ge, Si -STW

The synchrotron powder diffraction data of 4BDMI-Si,Ge-STW with Ge_f=0.5 was indexed in space group $P6_122$ with a= 12.22 and c=30.21 Å. The structure was refined using GSAS[3] under the EXPGUI interface[4], starting from a model based on our published structure of calcined pure silica HPM-1[5]. This model was modified to have the unit cell parameters given above and Si and Ge initially in equimolar amounts in each tetrahedral site of the framework. Initially, soft restrains were imposed on T-O (T=Si or Ge, 1.675 Å) and O-O (2.730 Å) distances. These distances were derived from the corresponding distances in quartz-type SiO_2 and GeO_2 and averaged to account for a Si/Ge ratio of 1. During the course of the refinement the weight of the restrains was gradually decreased and eventually eliminated. The powder data were corrected for absorption using the empirical equation of Lobanov and alte da Veiga[3]. The background was initially modeled with a shifted Chebyshev polynomial with 14 fixed terms. Towards the end of the refinement these terms were increased to 16 and refined. After the initial refinement of scale factor, unit cell parameters, Zero and profile coeficients[6], the tetrahedral and oxygen atoms were allowed to move. Then fluoride was introduced in the D4R. With regard to the dication, we first attempted to model it as two halves, each half consisting of a dimethylimidazolium rigid body in the main zeolite cavity plus an ethyl satellite able to rotate along the bond linking it to the imidazolium. By constraining the distance between the end ethyl carbon of each half SDA it was expected that the dication could be properly modeled and refined. However, this would require refining 14 parameters of the rigid bodies, whereas only 9 can be refined in GSAS. Attempts to make incremental refinements (cyclically fixing some variables while refining the rest) proved unsuccessful. Additional attempts to refine in space group $P6_1$ (which has the same systematic absences and could avoid the existence of two symmetrical cations in space group $P6_122$) also failed. We then decided to refine the position and orientation of just a single dication as a unique rigid body, giving up the refinement of rotations around any C-C bond in the linker, and choosing one the conformations observed in the minimization study (see text). This strategy proved successful. The H atoms were not included and, instead, the fractional occupancy factors of each C attached to H was increased to account for the total amount of electrons in the CH, CH_2 or CH_3 groups. Then, the fractional occupancy of each T site by Ge and Si was refined (constrained to sum up to full occupancy), as well as the atom displacement parameters (constrained by type) and background polynomial coefficients.

Table S2 provides crystallographic and experimental parameters for the refinement, and the Rietveld plot is shown in Figure S5 and average bonds and angles are provided in Table S6.

Table S2. Crystallographic and experimental parameters for the Rietveld refinement of as-made 4BDMI- Ge,Si--STW.

Wavelength		0.56383 Å
Temperature		293K
2Θ Range		2.01-36.49 º
step		0.01 º
nº. of data points		3449
nº. of reflections		1181
Space group		*P6$_1$22*
Unit cell parameters (Å)		
	a,b	12.19692(22)
	c	30.1482(7)
	Cell Volume (Å^3)	3884.11(15)
Residuals:		
	R_p	3.87%
	R_{wp}	5.25%
	R_F^2	6.66%
	Reduced χ^2	4.965

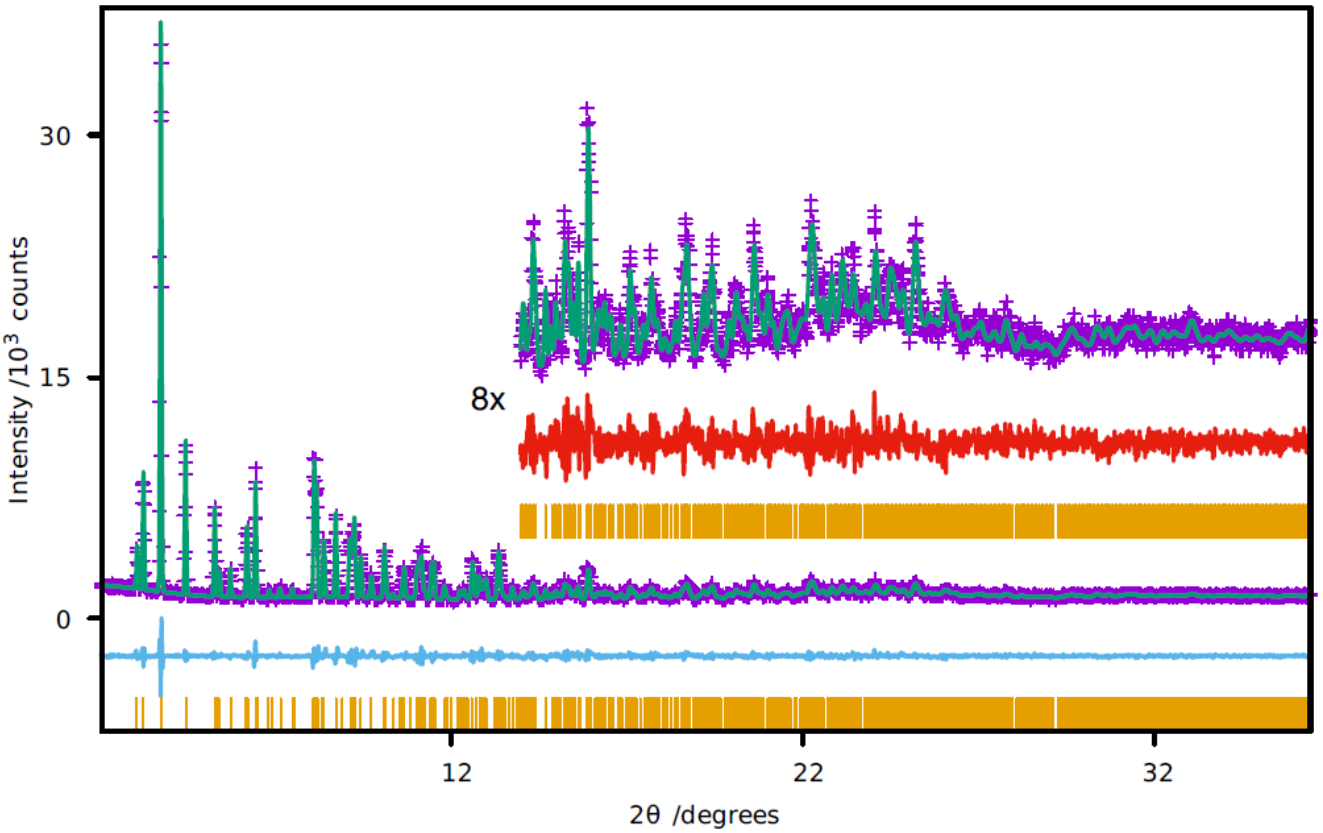

Figure S10. Observed (+) and calculated (solid line) powder X-ray diffractograms for as-made 4BDMI-Ge,Si-HPM-1 with nominal $Ge_f = 0.5$, refined in space group *P6₁22*. Vertical tic marks indicate the positions of allowed reflections. The lower trace is the difference plot. λ=0.56383 Å.

Table S3. Selected bonds and angles in 4BDMI-Ge,Si-HPM-1, obtained by Rietveld refinement.

Bond	**Average Distance (Å)**	**Atoms**	**Angle (ᵒ)**
T1-O	1.65	T5-O1-T5	164.7
T2-O	1.69	T1-O2-T2	135.6
T3-O	1.65	T4-O3-T5	132.9
T4-O	1.69	T5-O4-T5	149.2
T5-O	1.64	T3-O5-T5	132.2
T1-F	2.71	T1-O6-T1	143.1
T2-F	2.71	T2-O7-T4	141.2
T3-F	2.69	T1-O8-T3	136.3
T4-F	2.77	T1-O9-T4	144.0
Atoms	**Average Angle (ᵒ)**	T3-O10-T4	138.2
O-T1-O	109.4	T2-O11-T3	144.4
O-T2-O	109.3	T2-O12-T2	154.3
O-T3-O	109.1		
O-T4-O	109.0	Average T-O-T	143.0
O-T5-O	109.3		

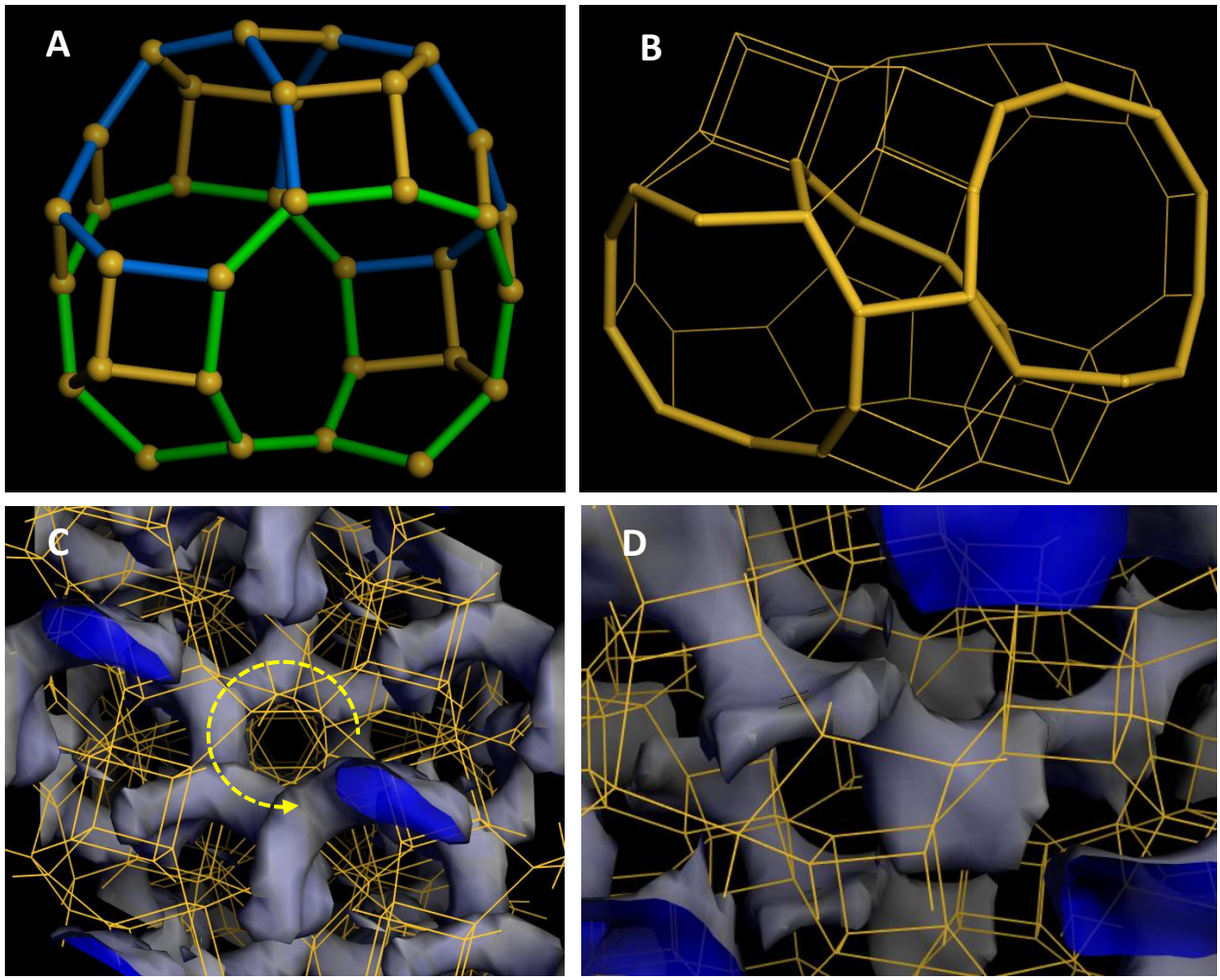

Figure S11. A: Asymmetry of the STW cavities, with 10-rings at one side (bottom side, highlighted in green) and 8-rings at the other side (top side, highlighted in blue). B: detail of how two cavities are connected (10-rings are highlighted as sticks). C: void volume showing the helicoidal channel. D: detail of the void volume in two consecutive cavities where the SDA dications will locate.

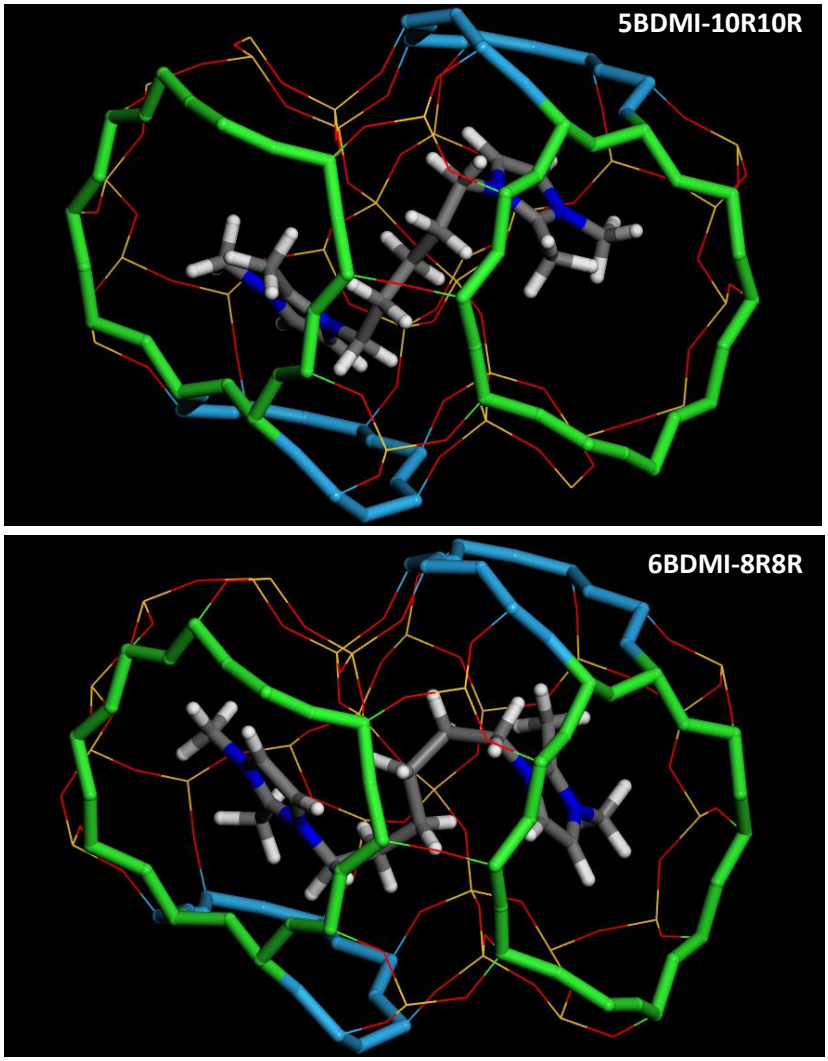

Figure S12. Location of 5BDMI in the less stable 10R10R configuration (top) and of 6BDMI in the less stable 8R8R configuration (bottom).

SDA	I.E. DFT	I.E. cvff	I.E. Dreiding
4BDMI	-1170.7	-527.7	-163.9
5BDMI	-1164.2	-517.3	-159.5
6BDMI	-1149.6	-470.5	-134.7

Table S4. Interaction energies (in kcal/mol per STW unit cell) for the different dications within the STW unit cell, as calculated by DFT, cvff or Dreiding methods.

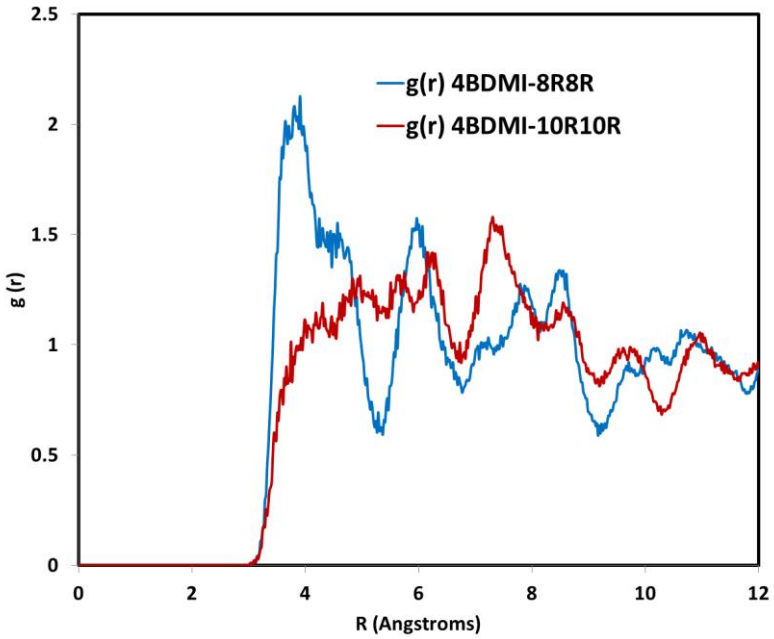

Figure S13. RDF between C(e) of 4BDMI and zeolite O atoms in two different configurations (8R8R in blue and 10R10R in red) during MD simulations.

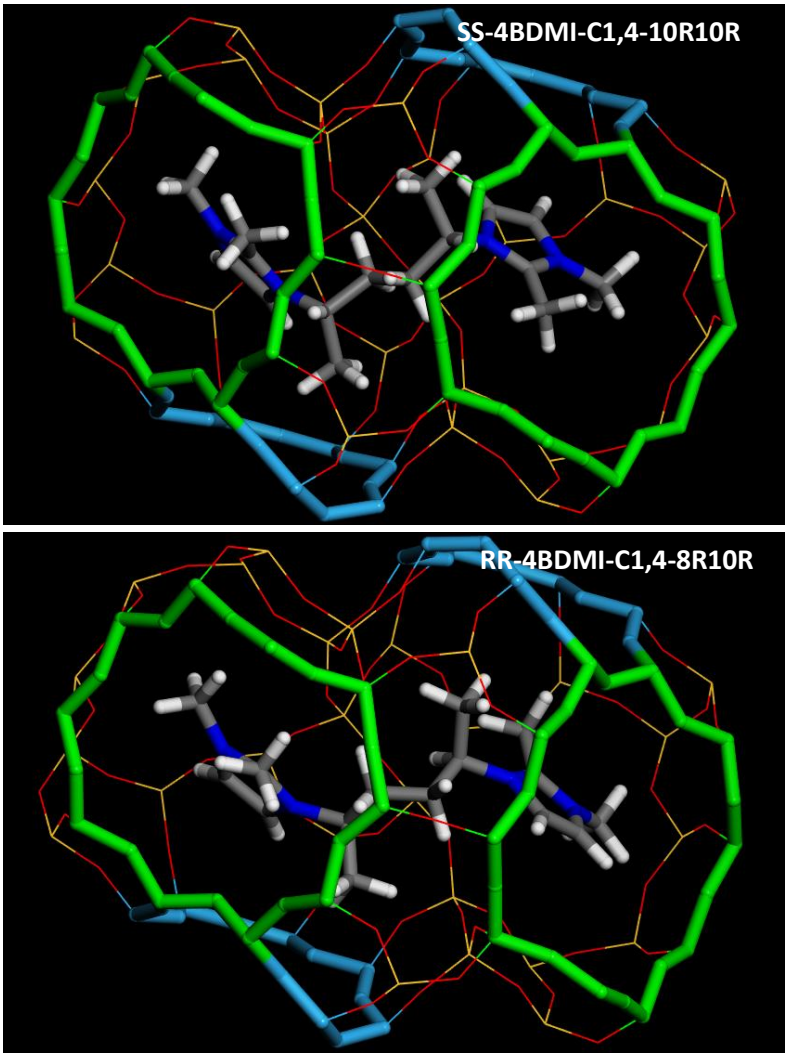

Figure S14. Location of of SS-4BDMI-C1,4 and RR-4BDMI-C1,4 in STW in the most stable configurations (10R10R for SS and 8R10R for RR, as determined by cvff).

References:

(1) Rojas, A.; Arteaga, O.; Kahr, B.; Camblor, M. A. *Journal of the American Chemical Society* 2013, *135*, 11975.
(2) Villaescusa, L. A.; Camblor, M. A. *Chemistry of Materials* 2016, *28*, 7544.
(3) Larson, A. C. *GSAS: Generalized Structure Analysis System*.
(4) Toby, B. *Journal of Applied Crystallography* 2001, *34*, 210.
(5) Rojas, A.; Camblor, M. A. *Angewandte Chemie International Edition* 2012, *51*, 3854.
(6) Thompson, P.; Cox, D. E.; Hastings, J. B. *Journal of Applied Crystallography* 1987, *20*, 79.